

# Ultrathin films of ferroelectric solid solutions under residual depolarizing field

Igor Kornev, Huaxiang Fu and L. Bellaiche

*Physics Department, University of Arkansas, Fayetteville, Arkansas 72701, USA*

(May 7, 2019)

## Abstract

A first-principles-derived approach is developed to study the effects of uncompensated depolarizing electric fields on the properties of  $\text{Pb}(\text{Zr},\text{Ti})\text{O}_3$  ultrathin films for different mechanical boundary conditions. A rich variety of ferroelectric phases and polarization patterns is found, depending on the interplay between strain and amount of screening of surface charges. Examples include triclinic phases, monoclinic states with in-plane and/or out-of-plane components of the polarization, homogeneous and inhomogeneous tetragonal states, as well as, peculiar laminar nanodomains.

Ferroelectric thin films are of increasing technological interest because of the need in miniaturization of devices [1]. An intriguing problem in these films concerns their polarization patterns. For instance, various patterns have been recently proposed from measurements, phenomenological theory and first principles. Examples are out-of-plane *monodomains* [2–5],  $180^\circ$  out-of-plane *stripe domains* [5,6],  $180^\circ$  and  $90^\circ$  multidomains that are oriented *parallel* to the film [7], and *microscopically-paraelectric* phases [4]. The fact that dramatically different patterns have been reported for similar *mechanical* boundary conditions supports a concept discussed in Refs [4,8,9], namely that they arise from different *electrical* boundary conditions. More precisely, real thin films are likely neither in ideal open-circuit conditions — for which unscreened polarization-induced surface charges can generate a large depolarizing electric field along the growth direction [10,11]— nor in ideal short-circuit conditions — that are associated with a vanishing internal field resulting from the full screening of surface charges —, but rather experience a situation in between. As a matter of fact, a reactive atmosphere can lead to a partial compensation of surface charges in films with nominal ideal open-circuit conditions [5], while metallic or semiconductor electrodes “sandwiching” films do not always provide *ideal* short-circuit conditions — resulting in a (non-zero) internal field, whose magnitude depends on the element from which these electrodes are made [4]. The *amount* of surface charges’ screening in thin films can thus vary from one experimental set-up to another, possibly generating *different* polarization patterns.

A precise correlation between this amount of screening and the morphology of the polarization pattern, and how this correlation depends on *mechanical* boundary conditions, are still lacking nowadays despite their obvious importance. Similarly, *atomic-scale* details of multidomains - and their formation mechanism - are mostly unknown in ferroelectric thin films. One may also wonder if some uncompensated depolarizing fields can yield unusual polarization pattern, such as monodomains made of ferroelectric phases that do *not* exist in the corresponding bulk material. Candidates for these latter anomalous features to occur are films made of perovskite alloys having a composition lying near their morphotropic phase boundary (MPB), because of the easiness of rotating their spontaneous polarization [12–15].

In this Letter, we develop a first-principles-based scheme to investigate the effects of uncompensated depolarizing fields on the properties of  $\text{Pb}(\text{Zr},\text{Ti})\text{O}_3$  films near their MPB, for different mechanical boundary conditions. Answers to the problems summarized above are provided. In particular, we find a rich variety of ferroelectric phases, including unusual triclinic and monoclinic states. We also observe complex nanodomains, and reveal their formation and atomic characteristics.

Specifically, our  $\text{Pb}(\text{Zr}_{1-x}\text{Ti}_x)\text{O}_3$  (PZT) thin films (i) are grown along the [001] direction (to be chosen along the z-axis); (ii) are “sandwiched” between non-polar systems (mimicking, e.g., air, vacuum, electrodes and/or non-ferroelectric substrates); (iii) have Pb-O terminated surfaces; and (iv) have a 50% overall Ti composition. Such low-dimensional structures are modeled by large periodic supercells that are elongated along the z-direction, and that contain a few number of B-layers to be denoted by  $m$  — with the alloyed atoms being randomly distributed inside each of these  $m$  planes. (The resulting films thus have a thickness  $\simeq 4m$  Å). Typically, we use  $10 \times 10 \times 40$  periodic supercells with  $m$  around 5. The non-polar regions outside the film are thus altogether  $40 - m$  lattice constant thick along the growth direction, which allows well-converged results for the films properties. The total energy of such supercell is used in Monte-Carlo simulations, and is written as:

$$\begin{aligned}
E_{tot}(\{\mathbf{u}_i\}, \{\mathbf{v}_i\}, \eta, \{\sigma_i\}) &= E_{Eff}(\{\mathbf{u}_i\}, \{\mathbf{v}_i\}, \eta, \{\sigma_i\}) \\
&- \sum_i \beta 2\pi \frac{Z^2}{a^3 \epsilon_\infty} \langle u_{j,z} \rangle_s u_{i,z}
\end{aligned} \tag{1}$$

where  $E_{Eff}$  is the (alloy effective Hamiltonian) energy of the ferroelectric film *per se*. Its expression and first-principles-derived parameters are those given in Ref. [14] for bulk PZT.  $\mathbf{u}_i$  are the local soft modes in unit cells  $i$  of the PZT film — which are directly proportional to the electrical polarization and whose components along the z-axis are denoted as  $u_{i,z}$ .  $\{\mathbf{v}_i\}$  are inhomogeneous strain-related variables inside these films [16], while  $\{\eta\}$  is the homogeneous strain tensor. As indicated in Ref. [17], the form of  $\{\eta\}$  (in Voigt notation) is relevant to two cases of interest, namely stress-free *vs.* epitaxially strained (001) films. In the former case, all the components of  $\{\eta\}$  fully relax. On the other hand, the second situation is associated with the freezing of three components of  $\{\eta\}$  — i.e.,  $\eta_6 = 0$  and  $\eta_1 = \eta_2 = \delta$ , with  $\delta$  being the strain resulting from the lattice mismatch between the film and the substrate — while the other components relax during the simulations [17].  $\{\sigma_i\}$  characterizes the atomic configuration, i.e.  $\sigma_i = +1$  or  $-1$  corresponds to the presence of a Zr or Ti atom, respectively, at lattice site  $i$  in the PZT film. The local modes and the inhomogeneous strain-related variables are forced to vanish in the supercell areas located outside the PZT films. Therefore, a depolarizing field implicitly occurs inside the film if this latter has a component of its polarization along the growth direction. The second term of Eq (1) mimics the effects of an *internal* electric field — that arises from the *partial or full screening* of polarization-induced charges at the *surfaces*, and that is thus opposite in direction to the *unscreened* depolarizing field — on the films properties. This energetic term is dependent on the  $Z$  Born effective charge [16], the  $a$  lattice constant, the  $\epsilon_\infty$  optical dielectric constant of  $\text{Pb}(\text{Zr}_{0.5}\text{Ti}_{0.5})\text{O}_3$ , and the average of the z-component of the local modes centered at the surfaces (denoted by  $\langle u_{j,z} \rangle_s$ , and that is self-consistently updated during the simulations) [18]. This second term is also directly proportional to a  $\beta$  parameter that characterizes the *strength* of the  $E_d$  *total* electric field inside the film. Specifically,  $\beta = 0$  corresponds to *ideal open-circuit* boundary conditions with  $E_d$  having its maximum magnitude (when polarizations lie along the z-axis), while an increase in  $\beta$  lowers this magnitude.

The value of  $\beta$  resulting in a vanishing total internal electric field is dependent on the supercell geometry, and in particular on the number of its non-polar layers [10]. This *ideal short-circuit*  $\beta$  is denoted as  $\beta_{SC}$  in the following. It is found to be 0.69, *for stress-free films associated with  $m = 7$  and a supercell periodicity of 40 lattice constant along the z-axis*, by fitting the  $T = 10$  K predictions delivered by Eq (1) to a single result of Ref. [3] (that constructed a microscopic Effective Hamiltonian for thin films under stress-free and ideal short-circuit boundary conditions); that is, the polarization in the film layer that is further away from the surfaces is along the z-axis and has a magnitude equal to the one in the bulk [19]. (Note that  $\text{Pb}(\text{Zr}_{0.5}\text{Ti}_{0.5})\text{O}_3$  *bulk* is tetragonal with an average local mode of 0.1072, in lattice constant units, at  $T=10$  K [14]). We found that our resulting  $T = 10$  K layer-by-layer profiles of the local modes for stress-free ultrathin films, that are under ideal short-circuit electrical boundary conditions, are remarkably similar to those of Ref [3]. For instance, the polarization at the surfaces is significantly enhanced with respect to the bulk, and increases as the film thickness decreases. Ref. [3] and our proposed scheme also both predict that the layers exhibiting the smallest polarization are those next to the surface layers, and that the layer that is further away from the surfaces has a larger polarization for  $m = 5$  than for

$m = 3$  or  $7$  (thus exhibiting a non-monotonic behavior versus thickness).

Having demonstrated that our approach can capture subtle details, we now apply it to study the effects of *uncompensated* depolarizing fields on the ground-state of  $\text{Pb}(\text{Zr}_{0.5}\text{Ti}_{0.5})\text{O}_3$  ultrathin films. The thickness is kept fixed at  $m = 5$ , while different *mechanical* boundary conditions are adopted: (a) stress-free (Fig 1a); (b) a tensile strain  $\delta = +2.65\%$ , corresponding to an increase of 0.02 Bohr for the in-plane lattice constant with respect to  $\text{Pb}(\text{Zr}_{0.5}\text{Ti}_{0.5})\text{O}_3$  bulk (Fig 1b); (c) a compressive strain  $\delta = -2.65\%$  (Fig 1c). More precisely, Figs 1 show the predicted (absolute value of the) Cartesian components  $\langle u_x \rangle$ ,  $\langle u_y \rangle$  and  $\langle u_z \rangle$  — along the [100], [010] and [001] directions, respectively — of the average of the local mode vectors in the film, as a function of  $\beta/\beta_{SC}$  and at  $T=10$  K. Figs 1 also display the behavior of  $u_M$ , which is defined as  $u_M = \sqrt{\langle u_x^2 + u_y^2 + u_z^2 \rangle}$  and thus provides a measure of the *local* polarizations.

Under *stress-free* conditions, the film has a spontaneous polarization *aligned along the z-axis* for (large) values of  $\beta$  that correspond to a screening of at least 98% of the polarization-induced surface charges. This results in a tetragonal state to be denoted by  $T_z$ . On the other hand, when  $\beta$  becomes smaller than  $\simeq 0.904\beta_{SC}$ , the internal field along the growth direction would be too strong to allow an out-of-plane component of the local mode. As a result, the polarization aligns along an *in-plane*  $\langle 010 \rangle$  direction. The corresponding ferroelectric phase is denoted as  $T_y$ . The most striking result for stress-free PZT films is the polarization path when going from  $T_z$  to  $T_y$ . As  $\beta/\beta_{SC}$  decreases from 98% to 90.4%, the polarization continuously rotates and passes through *three low-symmetry* phases: a so-called monoclinic  $M_A$  state [20] — occurring for  $0.932 \leq \beta/\beta_{SC} \leq 0.98$ , and for which  $\langle u_y \rangle$  and  $\langle u_x \rangle$  are nonzero, equal to each other and smaller than  $\langle u_z \rangle$ ; a triclinic  $Tr$  phase, for  $\beta/\beta_{SC}$  ranging between 92.2 and 93.2%, that is characterized by a local mode with non-zero and different Cartesian components; and a so-called monoclinic  $M_C$  ground-state [20], when  $\beta/\beta_{SC}$  ranges between 90.4 and 92.2%, for which  $\langle u_x \rangle$  vanishes while  $\langle u_y \rangle$  becomes larger than  $\langle u_z \rangle$ . Interestingly, neither the  $Tr$  nor the  $M_C$  phase exists in the temperature-versus-composition phase diagram of PZT bulk! Decreasing dimensionality thus leads to unusual phases because of residual depolarizing fields. Moreover, all the low-symmetry states of Fig 1a are only stable for compositions lying near the MPB of bulk PZT since we found that the  $M_A$ ,  $Tr$  and  $M_C$  phases disappear in favor of  $T_z$  for higher Ti concentration.

Comparing Fig. 1b with Fig. 1a reveals that films under a *tensile* strain react to depolarizing fields in a dramatically different way than stress-free films. In particular, the end-member phases ( $T_z$  and  $T_y$ ) of Fig 1a both disappear. The reason for the vanishing of the (ideal-short-circuit-derived)  $T_z$  phase is that tensile strains favor in-plane components of the local modes, because of the well-known coupling between strain and polarization [16,17,21]. Consequently,  $T_z$  transforms into a  $M_A$  phase for large enough  $\eta_1 = \eta_2 = \delta$  strains. These epitaxial constraints — and more precisely the fact that  $\eta_2$  can *not* be different than  $\eta_1$  — generate an in-plane component of the polarization along the [100] direction in addition to a larger component along the [010] direction, for small  $\beta$ . The (ideal-open-circuit-derived)  $T_y$  state thus becomes a  $M_C$  phase when going from stress-free to tensile conditions [22].

Conversely, a large enough *compressive* strain annihilates the (in-plane)  $\langle u_x \rangle$  and  $\langle u_y \rangle$  components of the local mode for *any*  $\beta$  (see Fig. 1c). Two *macroscopically*-different phases result from this annihilation: a *paraelectric*  $P$  phase for  $\beta$  smaller than  $0.822\beta_{SC}$  and a ferroelectric tetragonal  $T_z$  phase for larger  $\beta$ .  $T_z$  can be further separated into two

*microscopically*-different phases. For  $\beta/\beta_{SC} \geq 0.884$ , the local polarizations all point along the growth direction and have similar magnitude, since  $\langle u_z \rangle$  is nearly equal to  $u_M$ . The resulting state is referred to as  $T_z^{(h)}$ . On the other hand, when  $\beta$  ranges between 82.2% and 88.4% of  $\beta_{SC}$ ,  $\langle u_z \rangle$  becomes smaller than  $u_M$ . This characterizes a locally-inhomogeneous polar state to be denoted by  $T_z^{(i)}$ . The transition between  $T_z^{(h)}$  and  $T_z^{(i)}$  is of first-order, as revealed by the sudden jump of both  $\langle u_z \rangle$  and  $u_M$ . Another striking feature that can be extracted from Fig. 1c when looking at  $\langle u_z \rangle$  and  $u_M$  is that the *macroscopically-paraelectric*  $P$  phase has a relatively large magnitude for its local polarizations!

In fact, Figs 1 tell us that the only phases for which the magnitude of the macroscopic polarization significantly differs from that of the local polarizations are  $T_z^{(i)}$  and  $P$ . Under thermal equilibrium, complex polarization patterns (if any) should thus only exist for compressively-strained *ultrathin* films, while large ferroelectric monodomains are likely to occur in ultrathin films that are under stress-free or tensile mechanical boundary conditions. In order to provide a detailed *microscopic* insight of compressively-strained thin films, Figs 2 (a), (b) and (c) display a snapshot of (very large)  $24 \times 24 \times 40$  supercell simulations yielding a  $T_z^{(h)}$ ,  $T_z^{(i)}$  and  $P$  phase, respectively. Fig 2(a) confirms that  $T_z^{(h)}$  is locally homogenous.  $T_z^{(h)}$  is likely the phase observed in Ref [2] since this latter also occurs for compressive strain and large screening of the surface charges. More striking, Fig 2(b) reveals that  $T_z^{(i)}$  is characterized by the formation of *nanodomains* having local dipoles that are aligned in an opposite direction with respect to the macroscopic polarization. These nanodomains propagate throughout the entire thickness of the film but are *laterally* confined. We believe that  $T_z^{(i)}$  is the phase experimentally seen in Ref [5], and denoted there as  $F_\gamma$ , since this latter exhibits features that are consistent with our inhomogeneous  $T_z^{(i)}$ , namely: (i) compressive strain conditions and *partially* compensated depolarizing fields; (ii) a non-zero spontaneous polarization along the z-axis; and (iii) broad diffraction peaks. In the  $P$  state (see Fig 2c), the nanodomains have laterally “percolated”, resulting in the formation of nanoscale  $180^\circ$  (out-of-plane) *stripe* domains. Such peculiar multidomains are consistent with the so-called  $F_\alpha$  and  $F_\beta$  phases observed in Ref [5]. Another interesting feature revealed by Fig. 2(c) — which is, to the best of our knowledge, the first atomic-scale picture of nanodomains in ferroelectric thin films — is that each domain is terminated at *one* surface with local dipoles aligned in opposite *in-plane* directions, while the other surface has *out-of-plane* dipoles. This contrasts with a commonly accepted picture of *out-of-plane*  $180^\circ$  domains in magnetic films for which *both* surfaces have *in-plane* magnetizations [23]. Finally, Fig. 2c also shows that the predicted period  $\Lambda$  of the laminar domains is  $\simeq 8a_{in}$ , where  $a_{in}$  is the in-plane lattice constant. This remarkably agrees with the measurements of Ref. [5] yielding  $\Lambda = 37\text{\AA}$  for compressively-strained  $20\text{\AA}$ -thick  $\text{PbTiO}_3$  films. (Other calculations we performed — using  $n \times n \times 40$  supercells with  $n=10, 16, 18, 20$  and  $24$  — confirm that  $\Lambda \simeq 8a_{in}$  or  $9a_{in}$ )

We thank D.D. Fong, R. Haumont, J. Junquera, I. Naumov, S.K. Streiffer and C. Thomson, for having stimulating our interest in the present topic. This work is supported by ONR grants N 00014-01-1-0365 and 00014-01-1-0600 and NSF grant DMR-9983678.

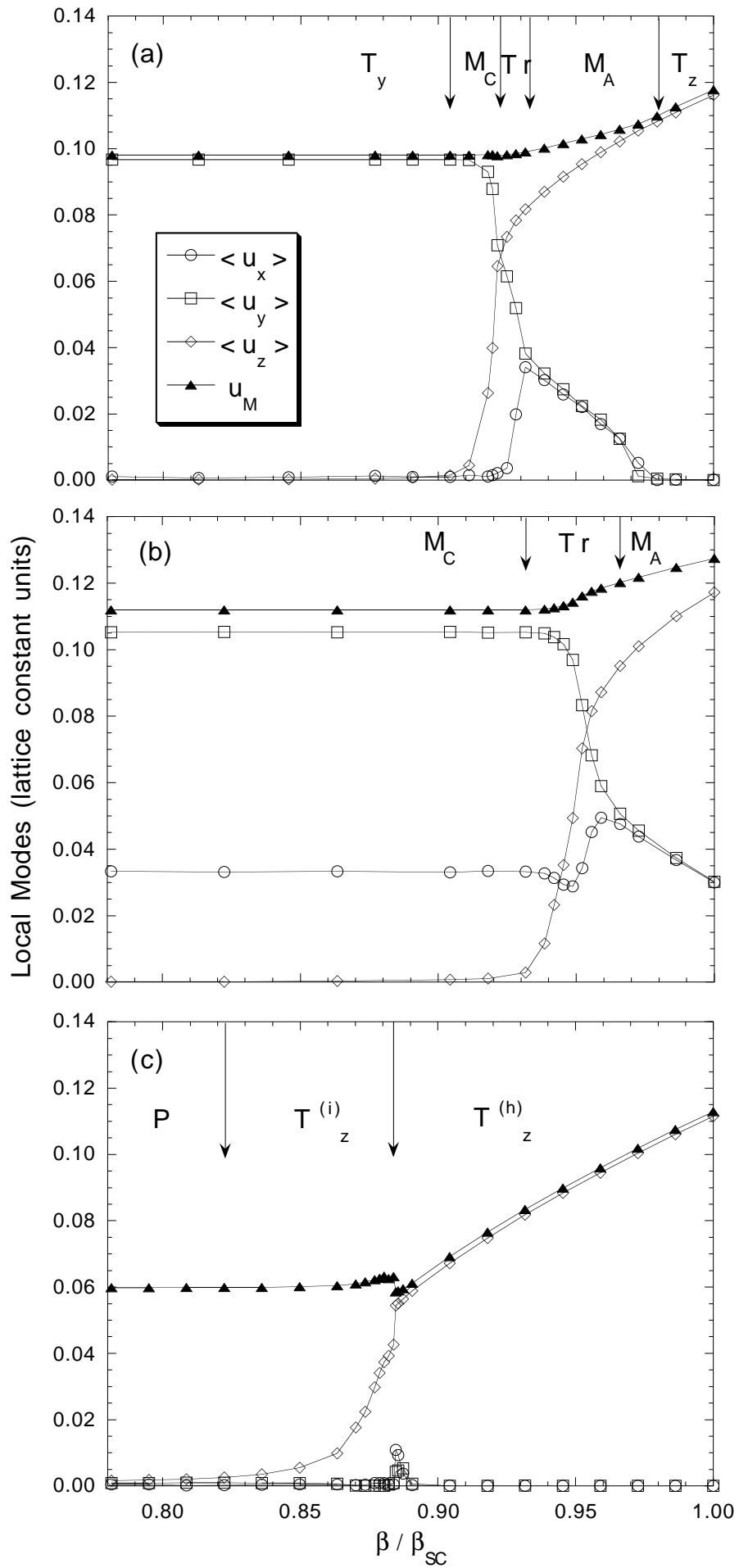
## REFERENCES

- [1] “Ferroelectric memories,” J.F. Scott, (Springer Verlag) (2000).
- [2] T. Tybell, C.H. Ahn and J.-M. Triscone, *Appl. Phys. Lett.* **75**, 856 (1999).
- [3] P. Ghosez and K.M. Rabe, *Appl. Phys. Lett.* **76**, 2767 (2000).
- [4] J. Junquera and P. Ghosez, *Nature* (London) **422**, 506 (2003)
- [5] S.K. Streiffer *et al.*, *Phys. Rev. Lett.* **89**, 067601 (2002).
- [6] A. Kopal, T. Bahnik and J. Fousez, *Ferroelectrics* **202**, 267 (1997).
- [7] Y. Drezner and S. Berger, *J. Appl. Phys.* **94**, 6774 (2003).
- [8] R.R. Mehta, B.D. Silverman and J.T. Jacobs, *J. Appl. Phys.* **44**, 3379 (1973).
- [9] J. Junquera *et al.*, *abstract of Fundamental Physics of Ferroelectrics 2004*, 86 (2004).
- [10] B. Meyer and D. Vanderbilt, *Phys. Rev. B* **63**, 205426 (2001).
- [11] R.E. Cohen, *J. Phys. Chem* **57**, 1393 (1996); *Ferroelectrics* **194**, 323 (1997).
- [12] B. Noheda, *Current Opinion in Solid State and Materials Science* **6**, 27 (2002).
- [13] J-M. Kiat *et al.*, *Phys. Rev. B*, **65**, 064106 (2002).
- [14] L. Bellaiche, A. García and D. Vanderbilt, *Phys. Rev. Lett.* **84**, 5427 (2000); *Ferroelectrics* **266**, 41 (2002).
- [15] I. Kornev and L. Bellaiche, *Phys. Rev. Lett.* **91**, 116103 (2003).
- [16] W. Zhong, D. Vanderbilt and K.M. Rabe, *Phys. Rev. Lett.* **73**, 1861 (1994); *Phys. Rev. B* **52**, 6301 (1995)
- [17] O. Dieguez *et al*, *cond-mat* 0402101 (2004)
- [18] Decomposing the total energy of thin film experiencing uncompensated fields as a sum of one term depending on bulk parameters and a second term associated with internal field, as we do in Eq (1), has previously been proposed in Refs [4,9] and reproduces well direct first-principles *macroscopic* results [4]. Our present scheme can also capture detailed *atomic* features because, unlike Refs. [4,9], (i) finite size effects are included in both energetic terms of Eq (1), and (ii) our depolarizing field depends on polarization at the surface (as it should be).
- [19]  $\beta_{Sc}$  for other thickness is derived from the one associated with  $m = 7$  by a rule of three involving the number of non-polar (001) B-layers in the corresponding supercells. For instance,  $\beta_{Sc}$  is +0.774 and +0.732 for  $m=3$  and 5, when using  $n \times n \times 40$  supercells (with  $n$  being an integer).
- [20] D. Vanderbilt and M.H. Cohen, *Phys. Rev. B* **63**, 094108 (2001).
- [21] R.E. Cohen, *Nature* **358**, 136 (1992).
- [22] The disappearance of the  $T_z$  and the  $T_y$  phases under tensile conditions is a MPB feature, since it does not occur in PZT ultrathin films having higher Ti composition.
- [23] L. D. Landau and E. M. Lifschitz, *Electrodynamics of Continuous Media*, Pergamon Press (1984).

## FIGURES

FIG. 1. Cartesian components of the film average of the local-mode vectors, as a function of the  $\beta/\beta_{Sc}$  parameter in (001)  $\text{Pb}(\text{Zr}_{0.5}\text{Ti}_{0.5})\text{O}_3$  ultrathin films having a  $m = 5$  thickness, at  $T = 10\text{K}$ . Part (a) displays the predictions for stress-film films. Parts (b) and (c) show the results for a tensile and compressive strain of 2.65%, respectively. The arrows indicate the values of  $\beta/\beta_{Sc}$  around which phase transitions occur. The results for  $\beta/\beta_{Sc}$  down to zero are not shown since they are identical to those associated with the lowest values of  $\beta/\beta_{Sc}$  displayed here.  $10 \times 10 \times 40$  supercells are used.

FIG. 2. Three-dimensional polarization patterns in (001)  $\text{Pb}(\text{Zr}_{0.5}\text{Ti}_{0.5})\text{O}_3$  films having a  $m = 5$  thickness and that are under a compressive strain of  $-2.65\%$ , at  $T = 10\text{K}$ . Part (a), (b) and (c) corresponds to a  $\beta/\beta_{Sc}$  parameter of 94.5% ( $T_z^{(h)}$  phase), 87.7% ( $T_z^{(i)}$  phase) and 80.8% ( $P$  phase), respectively. The bottom of Fig. 2c shows the projection of the 3D picture into a X-Z plane. The red (respectively, blue) color indicates local dipoles having a positive (respectively, negative) component along the z-axis.  $24 \times 24 \times 40$  supercells are used.



This figure "Fig2.png" is available in "png" format from:

<http://arxiv.org/ps/cond-mat/0403484v1>